IEICE TRANS. COMMUN., VOL.E85–B, NO.12 DECEMBER 2002

PAPER

Dispersion Compensation for Ultrashort Light Pulse CDMA Communication Systems

Yasutaka IGARASHI[†], ***Student Member and*** **Hiroyuki YASHIMA**[†], ***Regular Member***

SUMMARY We investigate dispersion compensation using dispersion-compensating fibers (DCFs) for ultrashort light pulse code division multiple access (CDMA) communication systems in a multi-user environment. We employ fiber link that consists of a standard single-mode fiber (SMF) connected with two different types of DCFs. Fiber dispersion can be effectively decreased by adjusting the length ratios of DCFs to SMF appropriately. Some criteria for dispersion compensation are proposed and their performances are compared. We theoretically derive a bit error rate (BER) of ultrashort light pulse CDMA systems including the effects of the dispersion and multiple access interference (MAI). Moreover, we reveal the mutual relations among BER performance, fiber dispersion, MAI, the number of chips, a bandwidth of a signal, and a transmission distance for the first time. As a result, we show that our compensation strategy improves system performance drastically.

key words: *ultrashort light pulse CDMA, fiber dispersion, dispersion-compensating fiber, SMF-DCF link, pulse broadening*

1. Introduction

In long distance optical transmission, single-mode fiber (SMF) is employed as a transmission medium. Since fiber loss does not limit transmission distance any longer on account of the introduction of Er-doped fiber amplifiers working over 1550-nm wavelength range, fiber dispersion is regarded as a main factor in limiting transmission distance and degrading system performance. Lately, various devices for dispersion compensation have been developed, and various techniques for the compensation have been studied to improve optical fiber transmission in time division multiplexing (TDM) and wavelength division multiplexing (WDM) systems.

Ultrashort light pulse code division multiple access (CDMA) based on the encoding and decoding in frequency domain has been proposed as the multiplexing technique in which unique code sequences are assigned to each user pair [1]. In ultrashort light pulse CDMA systems, fiber dispersion would be a main factor in degrading system performance. Since the light source of ultrashort light pulse CDMA system has wide bandwidth, it is supposed that the dispersion all over a total bandwidth would limit the transmission distance even if the dispersion could be compensated at a specific wavelength.

Manuscript received February 14, 2001.
Manuscript revised October 11, 2001.

[†]The authors are with the Department of Information and Computer Sciences, Saitama University, Saitama-shi, 338-8570 Japan.

So far, some researches on ultrashort light pulse CDMA have been presented. In [1], a bit error rate (BER) of ultrashort light pulse CDMA communication systems has been theoretically analyzed. Upper bounds and an approximation on the BER for ultrashort light pulse CDMA systems have been analyzed [2], then optical pulse position modulation signaling has been applied to ultrashort light pulse CDMA and its BER has been theoretically analyzed [3]. However, the dispersion compensation has not been studied in [1]–[3]. Meanwhile, experiments on an ultrashort light pulse CDMA system have been demonstrated in single-user system environment [4], where the dispersion is compensated in a fiber link and a receiver. However, a length of fiber link has been limited and fixed at 2.5-km, then system performance have not been theoretically analyzed.

Moreover, multiple access interference (MAI) from undesired users is also a factor of the performance degradation in ultrashort light pulse CDMA. Especially, when the dispersion is well compensated, MAI may be a dominant factor of the degradation. However, the theoretical analysis has not been presented for the ultrashort light pulse CDMA systems affected by both the dispersion and MAI.

In this paper, we theoretically analyze the performance of ultrashort light pulse CDMA communication systems including the dispersion compensation and MAI, and then evaluate its BER performance. This is the first work that studies the dispersion effect theoretically in ultrashort light pulse CDMA systems. Our study makes performance evaluation possible on condition for various parameters, e.g. the number of users, a code length, a bandwidth, and a transmission distance etc.. We discuss the performance characteristics related to the dispersion as well as these parameters.

Moreover, we propose new criteria to sufficiently compensate the dispersion effects over a total wavelength range. We employ two different types of dispersion-compensating fiber (DCF), DCF1 and DCF2, to compensate the dispersion of SMF accurately. We derive the dispersion characteristics of SMF-DCF links based on the dispersion compensation criteria, and compare the system performances for the SMF-DCF links. In the comparison, an effective compensation criterion is found.

2. System Configuration

Figure 1 shows ultrashort light pulse CDMA communication network. The same bit rate and on-off keying (OOK) signaling are assumed for all users and the m-th ($1 \leqq m \leqq M$) transmitter and the m-th receiver are paired where M is the total number of users. Data signals are imprinted on unique code that is transmitted asynchronously to common channel. Therefore, each user suffers from MAI. A pair of ultrashort light pulse CDMA transmitter and receiver is fully shown in Fig. 2. The transmitter consists of an ultrashort pulse generator, a data generator, and a spectral phase encoder. An ultrashort pulse having wide bandwidth is multiplied by the data generator. When a data is "0," the ultrashort pulse is not transmitted to the encoder and the output of the encoder is zero. While, when a data is "1," the ultrashort pulse is transmitted to the encoder. The encoder multiplies each spectral component of the ultrashort pulse by a specific phase shift unique to each user. This phase shift is operated by a spectral phase code generator. The spectral phase code of the m-th decoder is complex conjugate to one of the m-th encoder. Therefore, the m-th decoder reassembles only the signals from the m-th encoder properly, while it does not reassemble the signals from other encoders.

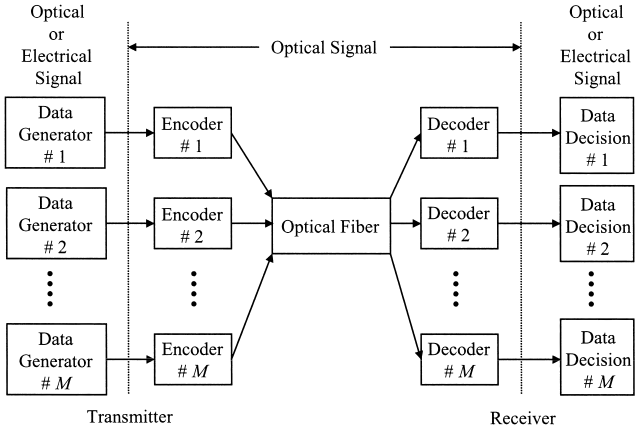

Fig. 1 Ultrashort light pulse CDMA communication network.

The practical structure of ultrashort light pulse CDMA is shown in Fig. 3. The spectral encoder is composed of a pair of diffraction gratings and confocal lens with a spatial phase mask. The ultrashort pulse representing one information bit is incident on the encoder through a data generator. The first grating spatially decomposes ultrashort pulse into its spectral

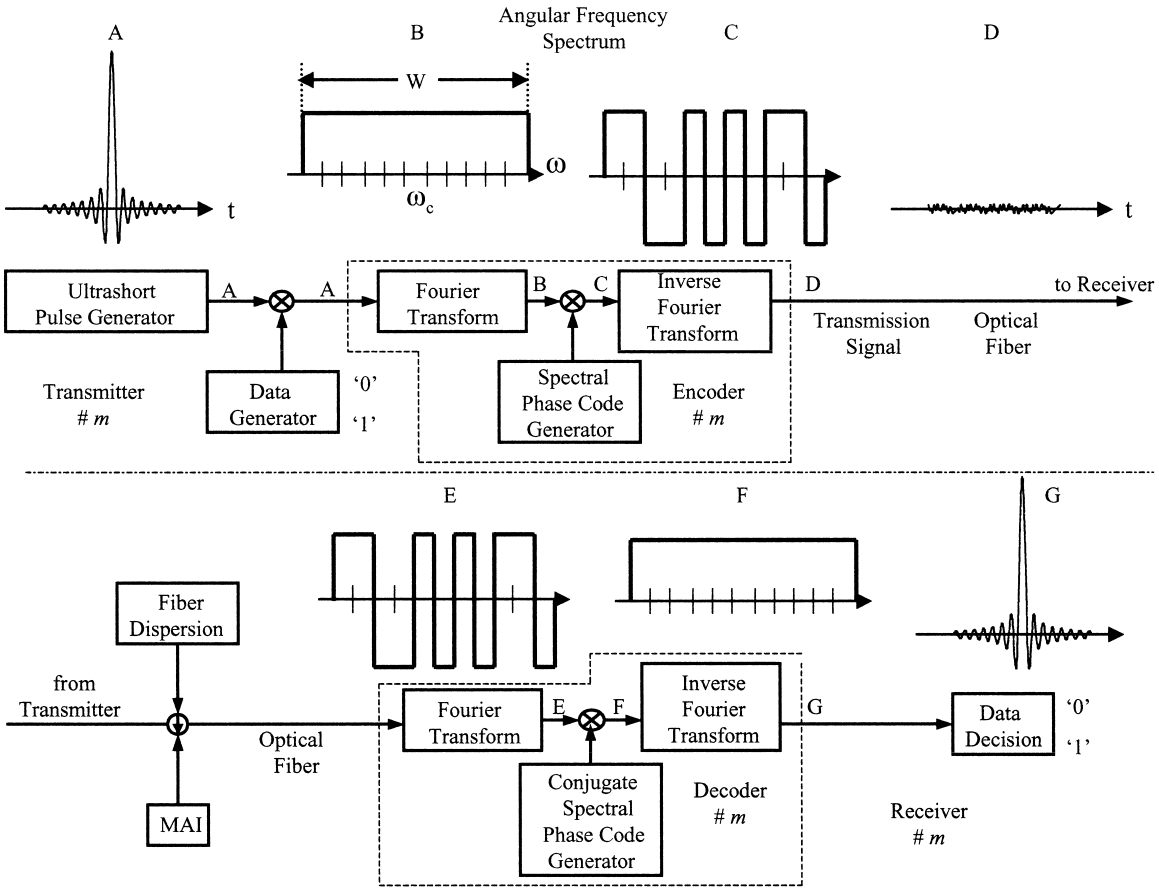

Fig. 2 Ultrashort light pulse CDMA transmitter and receiver.

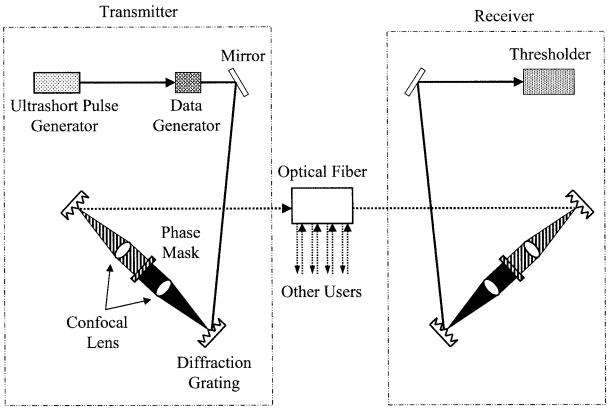

Fig. 3 The practical structure of ultrashort light pulse CDMA.

components. The spatial phase mask patterned pseudo-randomly applies pseudo-random phase shift to each spectral component. Therefore, high intensity ultrashort pulse is converted into low intensity pseudo-noise burst, whose waveform is given by the inverse Fourier transform of the pseudo-random mask pattern as shown in Fig. 2. The second grating recomposes the spectral components into the concentrated optical beam. A receiver consists of a spectral decoder, which is similar to the encoder, and a thresholder. When the encoding and decoding masks are a complex conjugate pair, the encoded signal is properly decoded, i.e. the decoding mask removes the pseudo-random phase shifts from the spectral components of the encoded signal and reassembles the original ultrashort pulse. On the other hand, when the encoding and decoding masks are not the matched pair, the decoding mask does not remove the pseudo-random phase shifts. Thus, the decoded signal remains the pseudo-noise burst. The thresholder detects the properly decoded ultrashort pulse and rejects the improperly decoded pseudo-noise burst.

Figure 4 shows encoding and decoding of ultrashort light pulse. Temporal waveform of the ultrashort pulse has an intensive spike. Angular frequency spectrum of the ultrashort pulse is characterized by baseband Fourier spectrum $A(\omega)$ given by

$$A(\omega) = \begin{cases} \frac{\sqrt{P_0}}{W}, & (|\omega| \leqq \frac{W}{2}) \\ 0, & (\text{elsewhere}) \end{cases} \tag{1}$$

where ω is angular frequency, P_0 is the peak power of the ultrashort pulse, and W is the total bandwidth of the Fourier spectrum. The encoder multiplies $A(\omega)$ by the phase code. The phase code consists of some chips, $N_0 = 2N+1$ is the total number of the chips, i.e. a code length. The bandwidth of the chip is $\Omega = W/N_0$. The example of the phase code ($N_0 = 11$) is illustrated in Fig. 4. The electric field representation of the encoded signals $E_m(t)$ at time t by the m-th encoder is expressed as follows [1]:

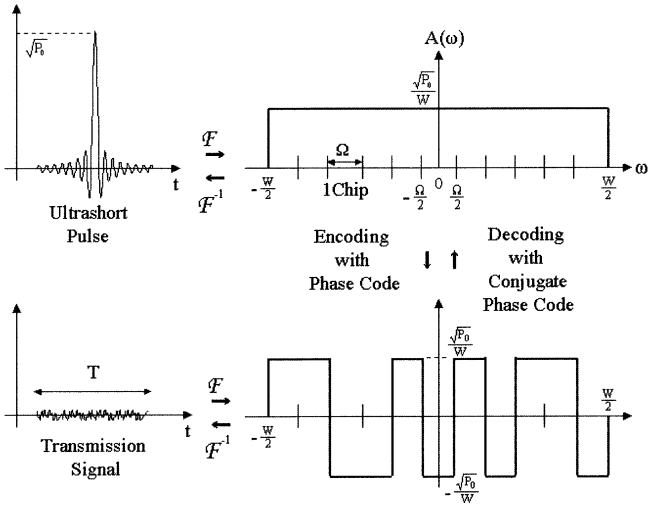

Fig. 4 Encoding and decoding of ultrashort light pulse. $\mathcal{F}$ and $\mathcal{F}^{-1}$ indicate Fourier transform and inverse Fourier transform, respectively.

$$E_m(t) = \sum_{j=-\infty}^{\infty} d_j^{(m)} V_m(t - jT_b) \tag{2}$$

where

$$V_m(t) = \frac{\sqrt{P_0}}{N_0} \sum_{n=-N}^{N} \exp\{-i(n\Omega t + \varphi_n^{(m)})\}, \quad \left(|t| \leqq \frac{T}{2}\right), \tag{3}$$

where $d_j^{(m)}$ is the data sequence produced by the m-th data generator and takes on either "0" or "1" for each j. $V_m(t)$ is the encoded pseudo-noise signal with a period T_b defined as the m-th address signal. Since the ultrashort pulse has a full-width at half-maximum (FWHM) of $\tau_c \simeq \frac{2\pi}{N_0\Omega}$, the duration of $V_m(t)$ is spread over $T = \frac{2\pi}{\Omega} \simeq N_0\tau_c$. Each user's bit rate is defined as $\frac{1}{KN_0\tau_c}$ where K is a ratio of T_b to T. $\varphi_n^{(m)}$ is the spectral phase code element of the n-th chip produced by the m-th code generator. The temporal waveform of $V_m(t)$ depends on the code elements. $\varphi_n^{(m)}$ is set to either 0 or π randomly with equal probability, i.e., $\exp(-i\varphi_n^{(m)})$ is set to either 1 or -1. The phase code sequences are assumed to be random sequences. Therefore, the encoded pseudo-noise signal and unsuccessfully decoded MAI can be modeled as the Gaussian random processes in this asynchronous CDMA system with many random access users for pure random coding [1].

3. Dispersion Compensation with DCF

We assume that the transmitted signals are plane waves polarized linearly and a polarized plane is always invariable and constant at the transmission channel. When a wide band signal travels through optical fiber, each

phase of frequency components of the signal is significantly shifted by fiber dispersion. If the phase codes for encoding and decoding are a complex conjugate pair, the decoder completely removes all the phase shifts operated by the encoder. However, the phase shift caused by fiber dispersion remains on each frequency component. Therefore, the decoded ultrashort pulse is distorted and broaden. This broadening pulse degrades the system performance. So, the dispersion compensation is a key issue in ultrashort light pulse CDMA system.

So far, some criteria of the dispersion compensation have been presented for optical TDM and WDM systems. In [5], the dispersion at a center wavelength is compensated to be zero. In [6], the maximum absolute value of the dispersion over the whole wavelength range is minimized. Also, the root mean square (rms) value of the dispersion is minimized for a W fiber [7].

In ultrashort light pulse CDMA system, even when the dispersion is compensated at a specific wavelength, the transmission distance would be still limited due to the residual dispersion on whole wavelength. Therefore, we propose some compensation criteria to reduce the dispersion over the total wavelength range.

Figure 5 shows an SMF-DCF link. The dispersion compensation technique we demonstrate here is to connect SMF with two DCFs, DCF1 and DCF2. Figure 6 shows the dispersion characteristics of SMF, DCF1, and DCF2. Since standard SMF has positive dispersion and dispersion slope at 1550-nm wavelength range, DCF is designed to have negative dispersion and dispersion slope for canceling out these of SMF simultaneously. Namely, the idea of the SMF-DCF link is to restore each shifted phase of the signal to the original by DCF. To compensate the dispersion as accurate as possible, we use two DCFs. Each of them has distinct dispersion characteristics. Before describing about our proposed compensation criteria, we derive average dispersion and average dispersion slope.

We denote that $\beta(\omega)$ is the propagation constant of optical fiber and z (> 0) is transmission distance. The phase shift $\phi(\omega, z)$ caused by fiber dispersion is given by

$$\phi(\omega, z) = -\beta(\omega)\, z. \tag{4}$$

$\frac{d}{d\omega}\beta(\omega)$ is defined as the group delay (inverse of group velocity) which is time for a frequency component to travel a unit length. The composite link of SMF and DCF can be regarded as the fiber link with the average propagation constant $\beta_{av}(\omega)$ given by

$$\beta_{av}(\omega) = \frac{\beta_{\rm SM}(\omega) + R_1\,\beta_{\rm DC1}(\omega) + R_2\,\beta_{\rm DC2}(\omega)}{1 + R_1 + R_2} \tag{5}$$

which is equivalent to the propagation constant averaged over total SMF-DCF link length. $\beta_{\rm SM}(\omega)$, $\beta_{\rm DC1}(\omega)$, and $\beta_{\rm DC2}(\omega)$ are the propagation constant for SMF, DCF1, and DCF2, respectively. R_1 and R_2 are the positive length ratio of the DCF1 to SMF and the DCF2 to SMF, respectively (see Fig. 5). $D(\lambda)$ and $D^{'}(\lambda)$ denote the dispersion and the dispersion slope of optical fiber at wavelength λ, respectively, given by

$$D(\lambda) = \frac{d}{d\lambda}\frac{d}{d\omega}\beta(\omega) \tag{6}$$

and

$$D^{'}(\lambda) = \frac{d}{d\lambda}D(\lambda). \tag{7}$$

From (5) and (6), the average dispersion $D_{av}(\lambda)$ is given by

$$D_{av}(\lambda) = \frac{D_{\rm SM}(\lambda) + R_1\,D_{\rm DC1}(\lambda) + R_2\,D_{\rm DC2}(\lambda)}{1 + R_1 + R_2} \tag{8}$$

where $D_{\rm SM}$, $D_{\rm DC1}$, and $D_{\rm DC2}$ are the dispersion for SMF, DCF1, and DCF2, respectively. Similarly, from (7) and (8), the average dispersion slope $D^{'}_{av}(\lambda)$ is given by

$$D^{'}_{av}(\lambda) = \frac{D^{'}_{\rm SM}(\lambda) + R_1\,D^{'}_{\rm DC1}(\lambda) + R_2\,D^{'}_{\rm DC2}(\lambda)}{1 + R_1 + R_2} \tag{9}$$

where $D^{'}_{\rm SM}$, $D^{'}_{\rm DC1}$, and $D^{'}_{\rm DC2}$ are the dispersion slope for SMF, DCF1, and DCF2, respectively. The rms value f of the average dispersion of the SMF-DCF link over the wavelength range between λ_1 and λ_2 is given by [7]:

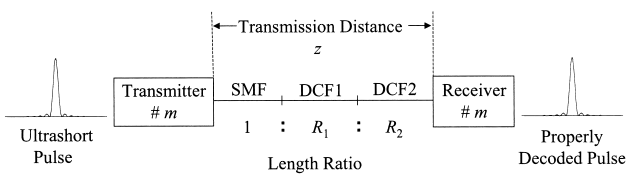

Fig. 5 Schematics of SMF-DCF link.

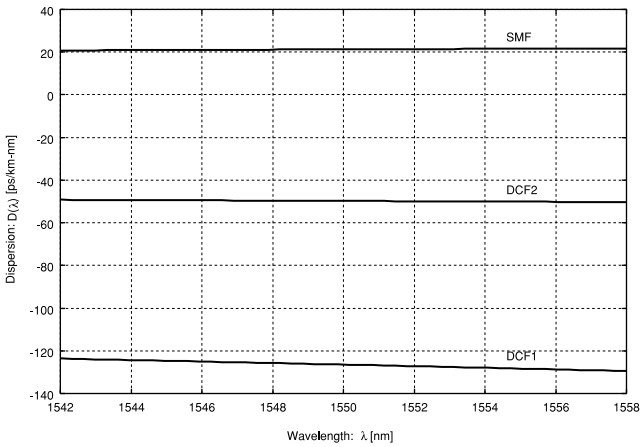

Fig. 6 Schematics dispersion characteristics of SMF, DCF1 and DCF2.

$$f = \sqrt{\frac{1}{\lambda_2 - \lambda_1} \int_{\lambda_1}^{\lambda_2} D_{av}^2(\lambda) d\lambda} \,. \tag{10}$$

Using (8)–(10), we propose three criteria to reduce the dispersion all over the SMF-DCF link. The BER performances are compared for these criteria. R_1 and R_2 are adjusted to satisfy the following criteria.

- A: satisfying $D_{av}^{'}(\lambda) = 0$ at center wavelength and minimizing f over the total wavelength range.
- B: satisfying both $D_{av}(\lambda) = 0$ and $D_{av}^{'}(\lambda) = 0$ at center wavelength.
- C: slightly changing R_1 and R_2 around each value obtained in A and B to achieve the maximum peak intensity of the properly decoded pulse.

The examples are shown in Sect. 5.

4. BER Analysis

The principal factors affecting BER are fiber dispersion, dispersion slope over a total wavelength range, and the undesired users' MAI appearing in multiple access channel. We assume that power levels in the fiber are sufficiently small so that we can neglect nonlinear effects as in [1]. Fiber loss is also ignored to focus on the effects of fiber dispersion and MAI. Moreover, the effects of quantum and thermal noise are small enough to ignore in this system. We also assume that the dispersion effect on the undesired users' MAI can be ignored†.

The temporal waveform of the properly decoded pulse $E(t, z)$ after traveling a distance of z can be given by the Fourier transform technique as:

$$E(t, z) = \mathcal{F}^{-1}\Big[A(\omega - \omega_c) \exp\{-i\phi_{av}(\omega, z)\}\Big] \tag{11}$$

where ω_c is the center angular frequency, $\mathcal{F}^{-1}$ is the inverse Fourier transform, and $\phi_{av}(\omega, z) = -\beta_{av}(\omega)\, z$ is the phase shift of the transmitted signals distorted by a little average dispersion in the SMF-DCF link. We assume $E_{kk}(t, z)$ to be the successfully decoded pulse sequences from the k-th encoder to the k-th decoder expressed as

$$E_{kk}(t, z) = \sum_{j=-\infty}^{\infty} d_j^{(k)} E(t - jT_b, z) \quad \Big(|t - (t'_{kk}(z) + jT_b)| \leqq \frac{T_b}{2} \Big) \tag{12}$$

where

$$t_{kk}^{'}(z) = \frac{\partial}{\partial \omega} \phi_{av}(\omega, z)\Big|_{\omega=\omega_c}. \tag{13}$$

Here $t_{kk}^{'}(z)$ denotes the time delay of the signal from the k-th encoder to the k-th decoder; a successfully decoded pulse $E(t - jT_b, z)$ has a peak when $t - jT_b = t_{kk}^{'}(z)$. $\phi_{av}(\omega, z)$ is the function characterized by the compensated SMF-DCF link. Since each user transmits the signal asynchronously in ultrashort light pulse CDMA system, the electric field representation of the k-th decoder's output $r(t, z)$ is given by

$$r(t, z) = E_{kk}(t, z) + \sum_{m \neq k} E_{mk}(t - t_{mk}^{'}) \tag{14}$$

where $E_{mk}(t)$ and $t_{mk}^{'}$ are the unsuccessfully decoded signal and the random time delay from the m-th encoder to the k-th decoder ($m \neq k$), respectively, i.e. the second term of the right side of (14) is the total MAI at the k-th decoder. The statistical characteristic of $E_{mk}(t)$ is identical to one of $E_m(t)$ because of the assumption of the random coding. To decide a data whether "0"or "1," we define $I(t, z)$ as the signal intensity given by

$$I(t, z) = r(t, z)\, r^{*}(t, z) \tag{15}$$

where * denotes complex conjugate. A data decision is carried out by comparing $I(t, z)$ with a threshold I_{th}. For a data signal format, desired sampling instants are at $t = t'_{kk} + jT_b$ $(j = 0, 1, 2, \ldots)$. At $|t - (t'_{kk}(z) + jT_b)| \leqq \tau_c/2$, $E_{kk}(t, z)$ is equal to either $E(t'_{kk}(z), z)$, when $d_j^{(k)}$="1," or 0, when $d_j^{(k)}$="0." In contrast, at $|t - (t'_{kk}(z) + jT_b)| > \tau_c/2$, $E_{kk}(t, z)$ is zero independent of $d_j^{(k)}$.

Subject to the assumption that the undesired l users have transmitted a data "1" at the desired sampling time, the conditional probability density function $P(I, t, z/d_j^{(k)}, l)$ of the signal intensity $I(t, z)$ is determined by a conditional joint probability density function $P_{r_x r_y}(r_x, r_y, t, z/d_j^{(k)}, l)$ where r_x and r_y are the real and imaginary parts of the received signal $r(t, z)$. Since r_x and r_y are modeled as the jointly Gaussian, the conditional joint probability density function is given by

$$P_{r_x r_y}(r_x, r_y, t, z/d_j^{(k)}, l) = \frac{1}{2\pi l\sigma^2} \exp\Big\{-\frac{(r_x - d_j^{(k)} E(t - jT_b, z))^2 + r_y^2}{2l\sigma^2}\Big\} \tag{16}$$

where $\sigma^2 = P_0/2N_0$. l is the random variable with a binomial distribution;

$$P(l) = \binom{M-1}{l} \Big(\frac{1}{2K}\Big)^l \Big(1 - \frac{1}{2K}\Big)^{M-1-l} \tag{17}$$

When $l = 0$, the probability density function reduces to

†We confirmed the dispersion effect on MAI. When the number of chips is small, the means and the deviations of MAI power are slightly different between the cases with and without the dispersion. However, the differences of these values can be neglected when the number of chips is sufficiently large, e.g. $N_0 \geqq 40$. Therefore, we keep the number of chips large enough to keep the validity of our assumption, which is reflected in the numerical result.

$$P_{r_x r_y}(r_x, r_y, t, z/d_j^{(k)}, l=0) = \delta(r_x - d_j^{(k)} E(t-jT_b, z))\delta(r_y), \quad (18)$$

and $P(I, t, z/d_j^{(k)}, l=0)$ is given by

$$P(I, t, z/d_j^{(k)}, l=0) = \delta(I - d_j^{(k)}|E(t-jT_b, z)|^2). \quad (19)$$

From (19), $I=0$, when $d_j^{(k)}$=0, and $I=|E(t-jT_b,z)|^2$, when $d_j^{(k)}$=1, are obtained. From (16), $P(I,t,z/d_j^{(k)},l)$ for $l \geqq 1$ is given by

$$P(I,t,z/d_j^{(k)},l) = I_0\Big(\frac{2N_0 d_j^{(k)}|E(t-jT_b,z)|\sqrt{I}}{lP_0}\Big) \cdot \frac{N_0}{lP_0}\exp\Big(-\frac{N_0}{lP_0}(I + d_j^{(k)}|E(t-jT_b,z)|^2)\Big) \quad (20)$$

where $I_0(x)$ is the modified Bessel function of the first kind and the zeroth order. When $d_j^{(k)}$="0," (20) at the proper sampling instants, $t = t_{kk}^{'}(z) + jT_b$, reduces to

$$P_I(I/d_j^{(k)}=0,\ l) = \frac{N_0}{lP_0}\exp\Big(-\frac{IN_0}{lP_0}\Big). \quad (21)$$

When $d_j^{(k)}$="1" and $t = t_{kk}^{'}(z) + jT_b$, (20) reduces to

$$P_I(I, z/d_j^{(k)}=1,\ l) = I_0\Big(\frac{2N_0|E(t'_{kk}(z),z)|\sqrt{I}}{lP_0}\Big) \cdot \frac{N_0}{lP_0}\exp\Big(-\frac{N_0}{lP_0}(I + |E(t'_{kk}(z),z)|^2)\Big). \quad (22)$$

At undesired sampling times ($|t - (t_{kk}^{'}(z) + jT_b)| > \frac{\tau_c}{2}$), (20) reduces to (21) independent of $d_j^{(k)}$, as $|E(t-jT_b,z)|^2 \simeq 0$ and $I_0(x) \simeq 1$ ($x \ll 1$).

Electronics in the receiver check the output of threshold device for the duration $\alpha\tau_c$ limited by the speed of the electronics. $\alpha = 1$ corresponds to the ideal device being active only at the moment when the desired signal is expected [1]. The receiver decides a data as "1" when $I(t,z)$ exceeds the threshold I_{th} at any time within an interval of the duration $\alpha\tau_c$ and as "0" otherwise. We assume that OOK is generated with equal probability 1/2. We derive the average probability of BER using the relation BER= $\langle \mathrm{BER}(l)\rangle_l$ where $\langle\cdot\rangle_l$ is ensemble average with respect to l. BER(l) is the conditional BER on l expressed as

$$\mathrm{BER}(l) = \frac{1}{2}\Big(P_1(l) + P_2(l)\Big) \quad (23)$$

where $P_1(l)$ is the probability that the signal intensity of the total MAI caused by the undesired l users exceeds the threshold alone at any of α sampling instants and $P_2(l)$ is the probability that the signal intensity of the sum of a data "1" signal from a desired user and the total MAI does not exceed the threshold. From (17) and (21)–(23), BER is given by

$$\begin{aligned}\mathrm{BER} &= \langle \mathrm{BER}(l)\rangle_l \\ &= \frac{1}{2}\sum_{l=1}^{M-1}\Big\{P(l)\Big(P_1(l)+P_2(l)\Big)\Big\} \\ &= \frac{1}{2}\sum_{l=1}^{M-1}\binom{M-1}{l}\Big(\frac{1}{2K}\Big)^l\Big(1-\frac{1}{2K}\Big)^{M-1-l} \\ &\quad \cdot\Big\{1-\gamma^{\alpha}(l)+\gamma^{\alpha-1}(l)\,\rho(l,z)\Big\}\end{aligned} \quad (24)$$

where

$$\gamma(l) = 1 - \int_{I_{th}}^{\infty} P_I(I/d_j^{(k)}=0,\ l)\,dI = 1 - \exp\Big(-\frac{I_{th}N_0}{lP_0}\Big) \quad (25)$$

and

$$\rho(l,z) = 1 - \int_{I_{th}}^{\infty} P_I(I, z/d_j^{(k)}=1,\ l)\,dI = 1 - Q\Big(|E(t'_{kk}(z),z)|\sqrt{\frac{2N_0}{lP_0}}, \sqrt{\frac{2N_0 I_{th}}{lP_0}}\Big). \quad (26)$$

Here, $Q(a,b)$ is Marcum's Q function defined as

$$Q(a,b) \equiv \int_b^{\infty} x\,\exp\Big(\frac{-a^2-x^2}{2}\Big)I_0(ax)\,dx. \quad (27)$$

5. Numerical Result

We show the numerical results of the average dispersion characteristics and BER for the compensated system obtained in the previous section. The compensation criteria are shown in Sect. 3. The center wavelength λ_c is set to 1550-nm, i.e. ω_c is set to 1.215×10^{15}-rad/s. $\beta_{av}(\omega)$ is expanded by Taylor expansion as follows:

$$\begin{aligned}\beta_{av}(\omega) &= \beta_{av}(\omega_c) + \frac{d}{d\omega}\beta_{av}(\omega)\Big|_{\omega=\omega_c}\cdot(\omega-\omega_c) \\ &\quad + \frac{1}{2!}\frac{d^2}{d\omega^2}\beta_{av}(\omega)\Big|_{\omega=\omega_c}\cdot(\omega-\omega_c)^2 \\ &\quad + \frac{1}{3!}\frac{d^3}{d\omega^3}\beta_{av}(\omega)\Big|_{\omega=\omega_c}\cdot(\omega-\omega_c)^3 \\ &\quad + \frac{1}{4!}\frac{d^4}{d\omega^4}\beta_{av}(\omega)\Big|_{\omega=\omega_c}\cdot(\omega-\omega_c)^4 + O(\omega^5)\end{aligned} \quad (28)$$

where $O(\omega^5)$ is a residue term over the fifth order and ignored in this calculation, since its effect is sufficiently small.

Figure 7 shows the average dispersion of the SMF-DCF link based on the criteria A, B, and C as shown in

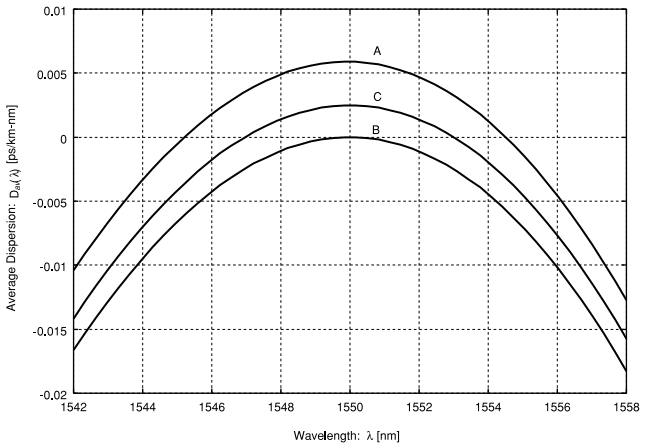

Fig. 7 Schematic average dispersion characteristics of connected SMF-DCF link. A : $R_1 \approx 0.16551$, $R_2 \approx 6.7945 \times 10^{-3}$. B : $R_1 \approx 0.16519$, $R_2 \approx 7.7427 \times 10^{-3}$. C : $R_1 \approx 0.16519$, $R_2 \approx 7.6840 \times 10^{-3}$.

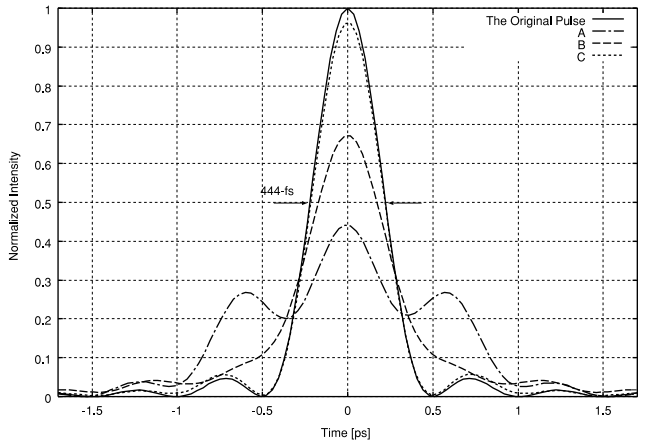

Fig. 8 The normalized intensity profiles of the properly decoded pulses passing through the SMF-DCF link of 33-km, $W \approx 1.26 \times 10^{13}$-rad/s. The curves A–C show the intensity profiles corresponding to the average dispersion curves A–C in Fig. 7, respectively. The solid line is the intensity of the original pulse with FWHM of 444-fs.

Sect. 3. A ($R_1 \approx 0.16551$, $R_2 \approx 6.7945 \times 10^{-3}$) is given by both satisfying $D'_{av}(\lambda_c) = 0$ and minimizing the rms value f in (10) at $\lambda_1 = 1542$-nm and $\lambda_2 = 1558$-nm. For B ($R_1 \approx 0.16519$, $R_2 \approx 7.7427 \times 10^{-3}$), the average dispersion and the average dispersion slope are completely compensated at 1550-nm by satisfying $D_{av}(\lambda_c) = 0$ and $D'_{av}(\lambda_c) = 0$. C is given by changing R_2 with fixed R_1 (≈ 0.16519) of B, to obtain the maximum peak intensity. As a result, we get $R_2 \approx 7.6840 \times 10^{-3}$ for the criterion C. As the length ratios change slightly, the dispersion curve shifts up or down significantly. Although the average dispersion characteristics are different for A–C, the dispersion slopes are almost the same.

Figure 8 shows the normalized intensity profiles of the properly decoded pulse that are calculated with (1), (5), (11) and (13) for $z = 33$-km and $W \approx 1.26 \times 10^{13}$-rad/s assuming the original pulse centered at 1550-nm with 444-fs FWHM duration. Pulse shapes are shown for the SMF-DCF links with A–C corresponding to the average dispersion curves A–C in Fig. 7, respectively. The intensity profile of C exhibits very little distortion. Although the difference of the length ratio between B and C is very slight (approximately 0.76% for R_2), the peak intensity of B drops to approximately 70% of C. This indicates that the accurate adjustment of the fiber length ratio is needed to achieve good compensation performance. To relax the precise adjustment of fiber length, it is desirable to use the DCF with small negative dispersion and dispersion slope, or a liquid crystal modulator [4], [8] capable of fine tuning for a nearly compensated fiber link.

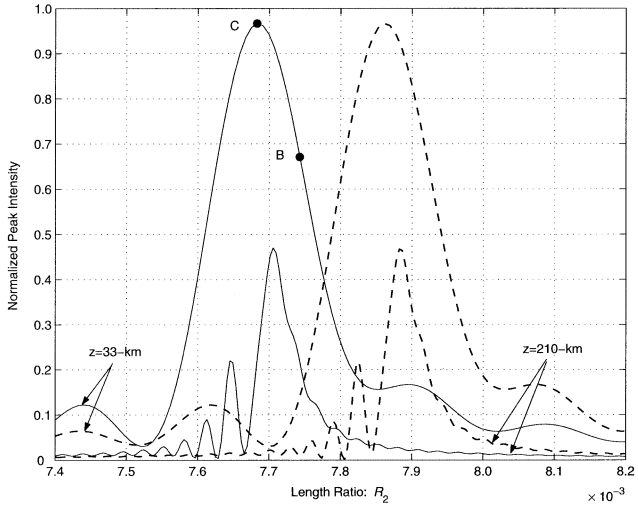

Fig. 9 The normalized peak intensity of the properly decoded pulse versus the length ratio R_2. Solid lines are for $R_1 \approx 0.16519$ and dashed lines are for $R_1 \approx 0.16512$.

Moreover, we search the optimum R_1 and R_2 to achieve larger peak intensity. Figure 9 shows the normalized peak intensity of the properly decoded pulse versus the length ratio R_2 that is calculated with (1), (5), (11), and (13) for $W \approx 1.26 \times 10^{13}$-rad/s. In this figure, the point B and C show the peak intensity given by the criterion B and C, respectively (see Fig. 8). Solid lines denote the normalized peak intensity for $R_1 \approx 0.16519$, which is given by the criterion B. Comparing the curves for $z = 33$-km and $z = 210$-km, the value of R_2 for the maximum peak intensity is slightly different. This shows that optimum length ratio depends on the transmission distance. With computer search around the value of R_2 given by the criterion B, the curve C in Fig. 7 is obtained by adjusting R_2 so as to achieve the maximum peak intensity at $z = 33$-km. Although solid lines and dashed lines have different value of R_1, almost the same maximum peak intensity could be achieved by adjusting R_2 properly. Therefore, it can be said that the optimum ratios R_1 and R_2 for the compensation are not only one pair. Indeed the

criteria A and B seem to be suitable criteria, but they are not derived from the optimum conditions. On the other hand, the criterion C is to fine-tune the length ratios with computer search around the values given by the criteria A and B. Therefore, the criterion C gives better result than the criteria A and B do.

Figure 10 shows BER versus transmission distance. BER is calculated by using (24)–(27) for $M = 5$, $K = 100$, $N_0 = 129$, $\alpha = 1$, $P_0 = 4$, $W \approx 1.26 \times 10^{13}$-rad/s, and each user's bit rate is 175-Mbit/s. We set $I_{th} = |E(t_{kk}^{'}(z), z)|^2/4$ that is the optimum threshold including the waveform distortion caused by the dispersion. BER of 1×10^{-9} can be achieved at $z \approx$ 22-km, 31-km, and 105-km for A, B, and C, respectively. The curve C shows almost flat BER characteristics within $z \approx$10-km. In this transmission distance range, the dispersion effect can be neglected, i.e. the system performance is substantially degraded by MAI. However, the dispersion effect substantially tends to dominate the error performance as a transmission distance gets longer.

Figure 11 shows BER versus transmission distance with the criterion C for $W \approx 9.41 \times 10^{12}$-rad/s, 1.26×10^{13}-rad/s and 1.57×10^{13}-rad/s corresponding to pulse durations of 592-fs, 444-fs and 355-fs, respectively. Each user's bit rate is 131-Mbit/s, 175-Mbit/s and 218-Mbit/s for $W \approx 9.41 \times 10^{12}$-rad/s, 1.26×10^{13}-rad/s and 1.57×10^{13}-rad/s, respectively. The other parameters are the same as for Fig. 10. The transmission distances to achieve BER=1×10^{-9} are about 43-km, 105-km and 333-km for $W \approx 1.57 \times 10^{13}$-rad/s, 1.26×10^{13}-rad/s and 9.409×10^{12}-rad/s, respectively. The transmission distance is drastically improved when W is small. This implies that the dispersion effect strongly increases as a bandwidth of the pulse increases.

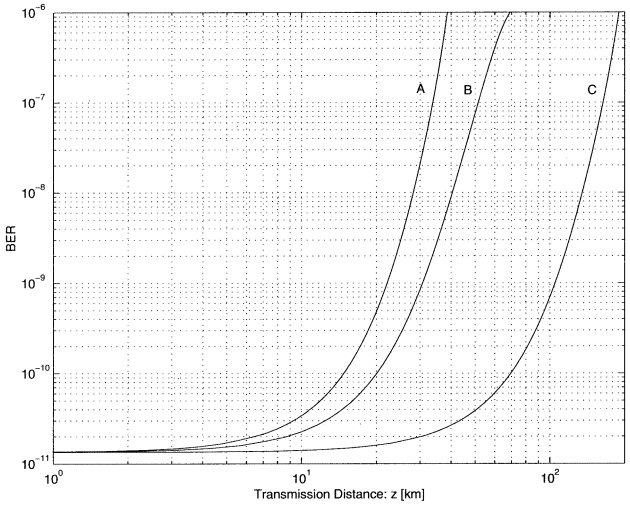

Fig. 10 BER versus transmission distance, $M = 5$, $K = 100$, $N_0 = 129$, $\alpha = 1$ and $P_0 = 4$. The curves A–C show the system performance corresponding to the average dispersion curves A–C in Fig. 7, respectively.

Figure 12 shows BER versus transmission distance with the criterion C for N_0=49, 77 and 121 corresponding to K=121, 77 and 49, respectively, so as to fix each user's bit rate at 380-Mbit/s. The other parameters are the same as for Fig. 10. The transmission distances for BER=1×10^{-7} are about 93-km and 139-km for N_0=77 and 121, respectively. For N_0=49, BER of 10^{-7} cannot be achieved because of MAI. Therefore, we should keep a code length as long as possible, which makes MAI power low.

Figure 13 shows BER versus transmission distance with the criterion C for M=5, 10, 20, 40, and 80. The other parameters are the same as for Fig. 10. Since the effect of MAI is large for a large number of users, BER of 10^{-8} cannot be achieved for M=40 and 80 even when

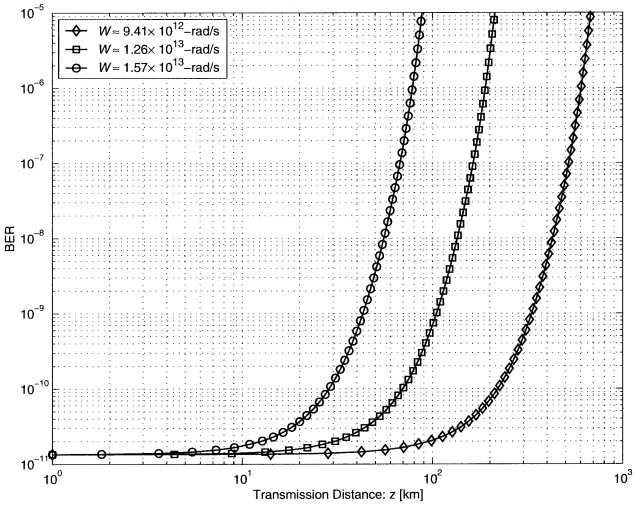

Fig. 11 BER versus transmission distance with the criterion C for $W \approx 9.41 \times 10^{12}$-rad/s, 1.26×10^{13}-rad/s and 1.57×10^{13}-rad/s corresponding to pulse durations of 592-fs, 444-fs and 355-fs, respectively.

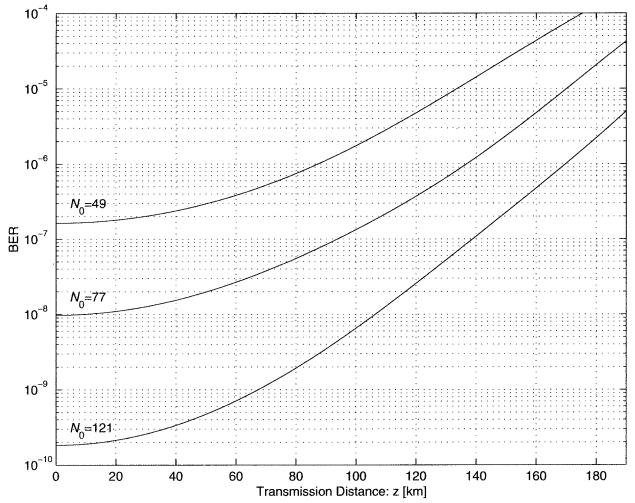

Fig. 12 BER versus transmission distance with the criterion C for N_0=49, 77 and 121 corresponding to K=121, 77 and 49, respectively, so as to fix each user's bit rate at 380-Mbit/s.

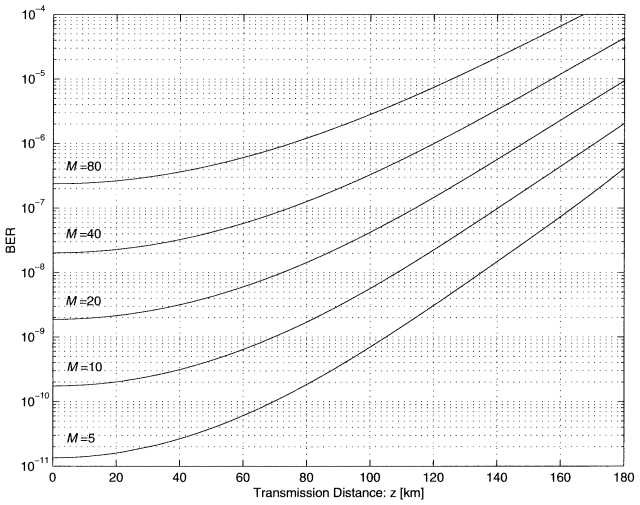

Fig. 13 BER versus transmission distance with the criterion C for M=5, 10, 20, 40, and 80.

the dispersion is well compensated. This shows that the effect of MAI on performance degradation cannot be ignored when the number of users is large.

6. Conclusion

We have investigated ultrashort light pulse CDMA communication systems with dispersion compensation. Two different DCFs are introduced into the SMF link for the accurate dispersion compensation. We propose two criteria of fiber dispersion compensation. Moreover, we search the optimum length ratios of DCFs. The BER performance of the compensated system is analytically derived. The numerical results show that the proposed dispersion compensation improves system performance drastically. It is found that the dispersion effect substantially increases as a transmission distance gets longer even in well compensated system. We also find that the system performance is substantially degraded by MAI for a short distance transmission when the dispersion is well compensated.

Acknowledgment

The authors would like to thank Prof. M. Takahara and Dr. M. Hanawa at Yamanashi University for helpful discussions. They also wish to thank Dr. E. Sasaoka, Dr. Y. Kajita, and Dr. S. Tanaka at Sumitomo Electric for providing the data of the DCF1 and DCF2.

References

[1] J.A. Salehi, A.M. Weiner, and J.P. Heritage, "Coherent ultrashort light pulse code-division multiple access communication systems," IEEE J. Lightwave Technol., vol.8, no.3, pp.478–491, March 1990.
[2] D.J. Hajela and J.A. Salehi, "Limits to the encoding and bounds on the performance of coherent ultrashort light pulse code-division multiple-access systems," IEEE Trans. Commun., vol.40, no.2, pp.325–336, Feb. 1992.
[3] K. Kamakura, T. Ohtsuki, and I. Sasase, "Optical spread time CDMA communication systems with PPM signaling," IEICE Trans. Commun., vol.E82-B, no.7, pp.1038–1047, July 1999.
[4] H.P. Sardesai, C.-C. Chang, and A.M. Weiner, "A femtosecond code-division multiple-access communication system test bed," IEEE J. Lightwave Technol., vol.16, no.11, pp.1953–1964, Nov. 1998.
[5] H. Izadpanah, C. Lin, J.L. Gimlett, A.J. Antos, D.W. Hall, and D.K. Smith, "Dispersion compensation in 1310 nm-optimised SMFs using optical equaliser fibre, EDFAs and 1310/1550 nm WDM," Electron. Lett., vol.28, no.15, pp.1469–1471, July 1992.
[6] A. Goel and R.K. Shevgaonkar, "Wide-band dispersion compensating optical fiber," IEEE Photon. Technol. Lett., vol.8, no.12, pp.1668–1670, Dec. 1996.
[7] R. Lundin, "Dispersion flattening in a W fiber," Appl. Opt., vol.33, no.6, pp.1011–1014, Feb. 1994.
[8] S. Shen and A.M. Weiner, "Complete dispersion compensation for 400-fs pulse transmission over 10-km fiber link using dispersion compensating fiber and spectral phase equalizer," IEEE Photon. Technol. Lett., vol.11, no.7, pp.827–829, July 1999.

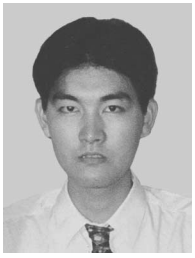

Yasutaka Igarashi was born in Tokyo, Japan, in 1975. He received the B.S. and M.S. degrees in information and computer science engineering from Saitama University, Japan, in 2000 and 2002. He is currently pursuing the Ph.D. degree in information and computer science engineering at Saitama University. His research is involved with optical code division multiple access (CDMA) communication systems and fiber dispersion compensation.

Hiroyuki Yashima was born in Mie, Japan, in 1958. He received the B.E., M.E., and Ph.D. degrees from Keio University, Japan, in 1981, 1987, and 1990, respectively, all in electrical engineering. Since 1990, he has been with the Department of Information and Computer Sciences, Saitama University, Saitama, Japan, where he is currently an Associate Professor. From 1994 to 1995, he was a Visiting Scholar at the University of Victoria, Victoria, British Columbia, Canada. His research interests include modulation and coding, optical communication systems, satellite communication systems, and spread spectrum communication systems. Dr. Yashima received the 1989 Society of Satellite Professionals International Scholarship Award.